Methods"; Ivin, K. J., Ed.; Wiley: New York, 1976; p 91 ff.
(8) Siegel, D.; Sixl, H.; Enkelmann, V.; Wenz, G. *Chem. Phys.* **1982**, *72*, 201.
(9) Enkelmann, V. *Adv. Polym. Sci.* **1984**, *63*, 91.
(10) Baughman, R. H.; Chance, R. R. *J. Polym. Sci., Polym. Phys. Ed.* **1976**, *98*, 481.
(11) Wenz, G.; Müller, M. A.; Schmidt, M.; Wegner, G. *Macromolecules* **1984**, *17*, 837. (Also referred to as paper 1.)
(12) Yoon, D. Y.; Brückner, S. *Macromolecules* **1985**, *18*, 651.
(13) Furukawa, Y.; Tacheuchi, H.; Harada, I.; Tasumi, M. *Bull. Chem. Soc. Jpn.* **1983**, *56*, 392.
(14) Zannoni, G.; Zerbi, G. *J. Mol. Struct.* **1983**, *100*, 485.
(15) Zerbi, G.; Gussoni, M. *J. Chem. Phys.* **1964**, *41*, 456.
(16) It must be pointed out that rigorously speaking eq 1 applies to the general normal mode; however, in the present case the approximation is very good considering that the ratios between the cross and the diagonal force constants are very small[13-15] and that the relative differences between the eigenvalues and the K_q's are quadratic functions of those ratios.
(17) Allegra, G.; Flisi, U.; Crespi, G. *Makromol. Chem.* **1964**, *75*, 189.
(18) Flory, P. J. In "Statistical Mechanics of Chain Molecules"; Interscience: New York, 1969; Chapter 1 and Appendix G.
(19) Saitô, N.; Takahashi, K.; Yunoki, Y. *J. Phys. Soc. Jpn.* **1967**, *22*, 219.
(20) Ronca, G.; Yoon, D. Y. *J. Chem. Phys.* **1982**, *76*, 3295.
(21) Porod, G. *Monatsh. Chem.* **1949**, *80*, 251.
(22) Kratky, O.; Porod, G. *Recl. Trav. Chim. Pays-Bas* **1949**, *68*, 1106.
(23) Sharp, P.; Bloomfield, V. A. *Biopolymers* **1968**, *6*, 1201.

Conformational Statistics of Poly(methyl methacrylate)

M. Vacatello*† and P. J. Flory

IBM Research Laboratory, San Jose, California 95193. *Received March 25, 1985*

ABSTRACT: Conformational energy calculations have been carried out for monomeric and trimeric oligomers of PMMA and for four-bond segments (embracing two repeat units) embedded in stereoregular PMMA chains, including both isotactic (meso) and syndiotactic (racemic) stereoisomeric forms. All incident interactions were taken into account. In each conformational domain the energy was minimized with respect to all bond angles and torsion angles including the torsional rotation χ of the ester group about the bond joining it to the chain backbone. Although in most of the conformations the plane of the ester group tends to occur approximately perpendicular to the plane defined by the adjoining skeletal bonds, substantial departures occur when one of these bonds is in a gauche $\bar{g}$ state. In consequence of this departure from $\chi = 0$ or π, the energy of the $\bar{g}$ conformations is not excessive, as was originally concluded. The intradiad bond angle $\tau' = 124 \pm 1°$ in all conformations after energy minimization. The interdiad bond angle $\tau = 106°$ when both adjoining skeletal bonds are trans t, $\tau \approx 111°$ when one bond is t and the other g or $\bar{g}$, and $\tau \approx 116°$ when both are g or $\bar{g}$. The spatial configurations found to be of lowest energy for stereoregular chains are in excellent agreement with crystallographic studies on i-PMMA and with results of wide-angle X-ray scattering of s-PMMA. The backbone torsional angles for the various energy minima can be represented approximately by six discrete states that form the basis for a rotational isomeric state treatment. Conformations near trans are preferred; the preference is pronounced for s-PMMA. Characteristic ratios and their temperature coefficients calculated according to the six-state scheme are in satisfactory agreement with experimental results. Parameters used in these calculations follow directly from the conformational energy calculations; adjustments are not required.

Introduction

The conformations accessible to poly(methyl methacrylate) (PMMA) chains were investigated by Sundararajan and Flory[1] on the basis of a simple rotational isomeric state (RIS) scheme with each skeletal bond assigned to either the trans t or the gauche g conformation. The alternative gauche $\bar{g}$ state was dismissed on the grounds that steric repulsions between atoms of the ester group and groups attached to the neighboring substituted skeletal carbon C^α (see Figure 1) were found to be acute in this conformation. Additionally, the skeletal bond angle τ_k, defined in Figure 1, was assumed to be 110° irrespective of the conformations of the adjoining skeletal bonds.

The steric repulsions operative in the $\bar{g}$ conformation depend on the orientation of the ester group[2] specified by the angle χ_k that measures the torsion about the C^α–C* bond; see Figure 1. Orientations $\chi = 0$ or π, in which the plane of the ester group is perpendicular to the plane defined by the adjoining skeletal bonds, were originally considered[1] to dominate all other possibilities owing to influences of steric interactions involving the skeletal methylene groups. This premise appeared to be supported by infrared absorption spectra of syndiotactic PMMA[3] and of model compounds[4] in the 1050–1300-cm^{-1} region. On the other hand, dielectric and mechanical relaxation measurements[5] indicate a greater diversity of orientations for the side groups. Conformational energy calculations subsequently carried out by Sundararajan[2] show that relaxation of the restriction of χ to values of 0 and π may facilitate occurrence of the $\bar{g}$ state in the vicinity of $\phi = -100°$ to $-120°$ (see ref 6 on conventions pertaining to the signs of torsional angles ϕ). Furthermore, recent FTIR investigations[8,9] on hydrogeneous and deuterated PMMA samples cannot be reconciled with the two-state scheme used previously; additional gauche states for the skeletal bonds are required to account for these results.[8,9]

Recent calculations on polyisobutylene[10] demonstrate that reliable conformational analysis of disubstituted vinyl polymers requires explicit allowance for the variability of the bond angles with conformation and for orientation correlations between substituents separated by several bonds. We present in this paper the results of a conformational analysis of PMMA in which all the bond angles and torsion angles have been treated as free variables subject to optimization. Using the outcome of preliminary calculations on simple models as starting point, we have minimized the energies of all eligible regular conformations for both isotactic and syndiotactic PMMA. The results are discussed in terms of a six-state RIS scheme.

Energy Calculations

Intramolecular conformational energies were calculated as sums of contributions from bond angle deformations, inherent torsional potentials, nonbonded interactions be-

†Permanent address: Dipartimento di Chimica, Università di Napoli, Via Mezzocannone 4, 80134 Naples, Italy.

0024-9297/86/2219-0405$01.50/0

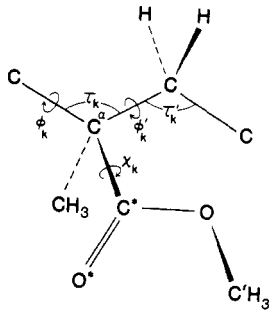

Figure 1. Structural unit of PMMA.

Table I
Parameters for Energy Calculation

bond	length, Å	intrinsic barrier, kcal mol^{-1}
C–C	1.53	2.80
C–C*	1.52	
C–H	1.10	
C*–O	1.36	8.75
C*=O*	1.22	
O–C′	1.45	1.55

bond angle	$k_\tau \times 10^3$, kcal mol^{-1} deg^{-2}	τ_0, deg
C–C–C	35.1	111
C–C–H	26.7	109.5
H–C–H	22.3	107.9
C–C*=O*	25.0	122
C–C*–O	30.7	114
O–C*=O*	49.5	124
C*–O–C′	28.5	110

atom	van der Waals radius, Å	effective no. of electrons	polarizability, Å^3	partial charge, esu
C	1.8	5	0.93	
H	1.3	0.9	0.42	
C*	1.8	5	1.23	0.517
O*	1.6	7	0.84	−0.417
O	1.6	7	0.70	−0.202
C′	1.8	5	0.93	0.102

tween pairs of atoms (separated by more than two bonds), and Coulombic interactions between partial charges appropriately assigned to atoms of the ester groups. Bond lengths were kept constant.

Energies E_τ of bond angle deformations were calculated in the usual quadratic approximation

$$E_\tau = (k_\tau/2)(\tau - \tau_0)^2 \qquad (1)$$

Bond lengths and values of k_τ and τ_0 for bond angles occurring in PMMA, taken from the literature[10-12] and used in the following calculations, are listed in Table I.

Distortion of bond angles vitiates the customary representation of the inherent torsional potentials by symmetric m-fold (e.g., threefold) sine functions. To overcome this difficulty, we assign a separate potential to each pair of atoms pendent to the bond considered. Thus, if X and Y are atoms attached respectively to A and B of the bond A–B, an m-fold potential that is symmetrical with respect to its minimum at the trans-periplanar conformation X-A-B-Y is assigned for this pair. The sum of the potentials for all such pairs, each referenced to the trans-periplanar conformation for that pair, is taken to represent the inherent torsional potential for bond A–B. For a C–C bond bearing six singly bonded substituents the magnitude of the barrier for each pair is $E_{CC}^0/9$, where we take E_{CC}^0 = 2.80 kcal/mol.[13] For O–C′ (see Figure 1) it is 1.55/3 kcal/mol,[14] and for the C*–O bond of the ester group it is taken to be 8.75/2 kcal/mol.[15] Although approximate, this procedure offers the advantage of consistency and should afford a significant improvement over assignment

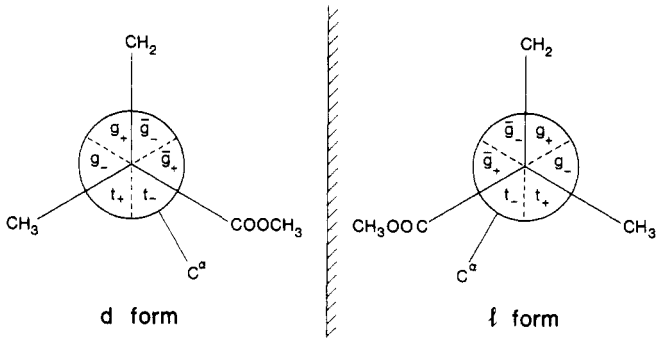

Figure 2. Conformations for enantiomeric d and l skeletal bonds of PMMA and their classification in six domains or states.

of a symmetric potential that fails to take account of the asymmetry resulting from bond angle deformations.

An inherent torsional potential for the C–C* bond was not included in the calculations. Microwave spectra of methyl acetate[16,17] indicate a threefold rotational potential with an energy barrier of only about 0.3 kcal/mol, its minima being located at the conformations in which C*=O* eclipses the C–H bonds. This feature is adequately reproduced by nonbonded interactions reckoned as described below, without resort to an inherent torsional potential for the C–C* bond.

Nonbonded interactions were evaluated as the sum of 6–12 Lennard-Jones potentials $E_{ij} = a_{ij}r^{-12} - b_{ij}r^{-6}$ for each atom pair ij separated by a distance r. The parameters b_{ij} were calculated from polarizabilities and effective numbers of electrons as detailed in ref 11. The a_{ij} were selected in such a way to make E_{ij} a minimum when r is the sum of the adjusted van der Waals radii for atoms i and j (see Table I). As discussed in ref 10, interactions with surrounding molecules can be taken into account approximately by letting $E_{ij}(r) = E_{ij}(r^*)$ for $r > r^* + h/2$, a cubic spline with the Lennard-Jones function being inserted for the range between $r^* - h/2$ and $r^* + h/2$ in order to avoid discontinuities of the first derivative of E_{ij} with respect to r. We select r^* = 4.5 Å and h = 1 Å.

Values given by Ooi et al.[18] for partial charges on the atoms of the ester group (see Table I) were used to evaluate the Coulombic interactions. In conjunction with the bond angles ∠CC*O* = 126°,[19] ∠CC*O = 111°,[19] and ∠C*OC′ = 113°,[11] these values reproduce the experimentally determined magnitude and direction of the dipole moment of the ester group in aliphatic compounds.[19] The effective dielectric constant was taken to be 3.5 for the estimation of Coulombic energies.

Calculations on Model Compounds

Staggered conformations in disubstituted vinyl polymers place groups bonded to successive quaternary carbon atoms (C$^\alpha$) at distances as small as 2.5 Å if the backbone angle τ_k' at the methylene group is assigned the tetrahedral value. When the substituents are carbon atoms or larger groups, the repulsive interactions are optimally alleviated by opening this angle and simultaneously displacing the torsional angles about the skeletal bonds from the values for perfect staggering. The magnitudes of these displacements depend on a delicate balance of the energies involved in all interactions and distortions at play.

With complete generality, we divide the 360° range describing rotations around the skeletal bonds into six equal intervals as shown in Figure 2. In conformity with the notation of ref 7, intervals in which C$^\alpha$ is placed syn to CH_3 and CH_2 are denoted by g, while those in which C$^\alpha$ is syn both to the ester group and to CH_2 are denoted by ḡ. The − and + subscripts in Figure 2 indicate the signs

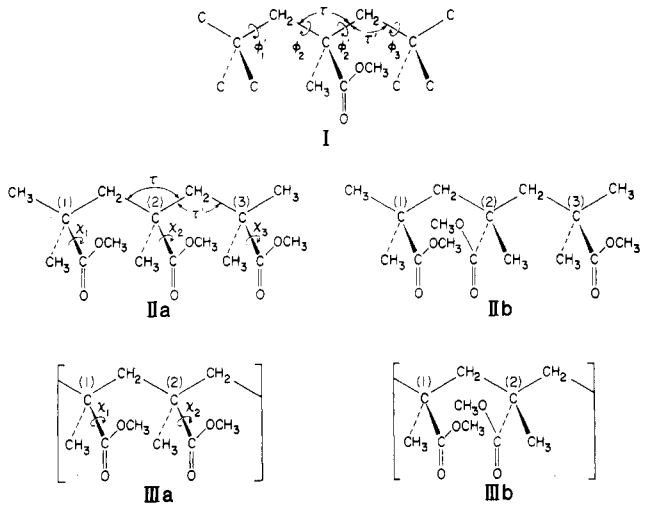

Figure 3. Model compounds and segments selected for the analysis of conformational energies.

of departure $\delta\phi$ from the respective locations (ϕ = 0°, 120°, and −120°) for perfect staggering of bonds that meet at the tetrahedral angle.

Opposite reference frames are affixed to *d* and *l* backbone bonds[6] identified in Figure 2. Accordingly, torsion angles about *d* bonds are reckoned in the right-handed sense while the left-handed sense is used for *l* bonds. The same convention applies to the signs of the $\delta\phi$'s. Hence, conformations of *d* and *l* bonds that are related by mirror reflection carry identical designations;[6,7] see Figure 2.

Relative to vinyl polymers having symmetrical substituents, the conformational analysis of PMMA is complicated by the presence of a substituent that is unsymmetrical with respect to rotation χ about the bond (C^{α}–C*) connecting it to the chain backbone; see Figure 1. The intramolecular energy therefore depends on this torsional angle as well as on torsional rotations (ϕ) about skeletal bonds. The usual procedure whereby the intramolecular energy associated with a given unit is represented by a surface that is a function of a pair of torsional angles is obviously inadequate here. Dependence on the torsional angle χ must be taken into account as well.

In order to simplify symbols required to specify the conformation and to rationalize their use, we identify the location of the *k*th α-carbon C^{α} along the chain by the serial index *k*. This index also identifies the *k*th interdiad junction. Then χ_k denotes the torsional rotation of the *k*th ester group as shown in Figures 1 and 3. In keeping with this notation we identify the torsion angles for the two bonds at the interdiad *k* by $\phi_k|\phi_k'$; see model I in Figure 3. The torsion angle around the C–C* bond and the CH_2–C–CH_2 bond angle at the same interdiad site are denoted by χ_k and τ_k, respectively. The intradiad bond angle following $C^{\alpha}{}_k$ is denoted by τ_k' and the intradiad torsional angles by $|\phi_k'\phi_{k+1}|$, as illustrated in Figure 3. The values of χ_k are measured in the sense dictated by the reference frame affixed to the second interdiad bond. Hence, the same set of values $\phi_k|(\chi_k)\phi_k'$ applies to a given interdiad conformation and to its mirror image in which the chiralities of the bonds at the interdiad and their conformations are inverted.

Model I. We first consider the simple model I shown in Figure 3. Computations were carried out by assigning initial values of 124° to the bond angles τ', as indicated by previous studies;[1] all other bond angles with the exception of those within the ester group were assigned the tetrahedral value of 109.5°. The bond angles of the ester group were fixed at the values quoted above. (These values follow also from the angles τ_0 given in Table I after allowing for the distortions due to repulsions between atoms attached to the subtended bonds.) For a given χ_2, the backbone torsion angles were assigned starting values corresponding to one of the 21 possible combinations of states (see Figure 2) that are nonequivalent by symmetry. The energy was then minimized with respect to ϕ_1', ϕ_2, ϕ_2', and ϕ_3 and to rotations of the methyl groups using quasi-Newton methods previously described.[10] Since ϕ_2 and ϕ_2' were not allowed to exit their respective domains, this calculation gives the minimum energy that can be obtained for each conformation of the backbone as a function of χ_2, with bond angles fixed at the values quoted.

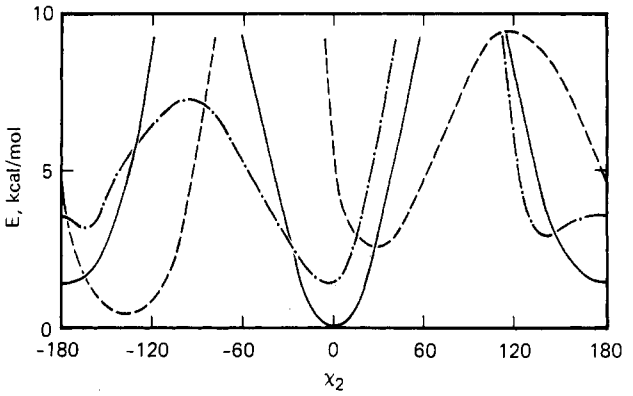

Figure 4. Energy minima as a function of the ester group torsion χ_2 in model I (Figure 3) for three skeletal conformations of the interdiad bond pair: $t_+|t_+$ (—); $t_+|\bar{g}_+$, (– – –); $t_-|g_+$ (–·–).

It will be evident that model I contains the minimum set of interactions generated in a PMMA chain as a consequence of the assignment of the interdiad couple (i.e., $\phi_2|\phi_2'$ in this model) to a given conformation. Additional attractive and repulsive contributions to the energy obviously are operative in an interdiad within a PMMA chain, inclusive of Coulombic interactions absent in model I. These additional interactions depend on ϕ_1' and ϕ_3 as well as on the stereochemical structure of the pair of diads. Nevertheless, conformations that are high in energy for model I are so because of interactions that occur also in the polymer.

As expected, conformations of I containing a g|g or a $\bar{g}|\bar{g}$ interdiad have exceedingly high energies for any value of χ_2. The origin of this observation is easily understood by examination of models; it has been fully discussed.[7,10] The energy for a $g_+|\bar{g}_-$ or $\bar{g}_-|g_+$ interdiad conformation also is large, although less than for g|g and $\bar{g}|\bar{g}$. In the course of minimization of the energy with respect to the skeletal torsional angles ϕ, a $g_+|\bar{g}_-$ or a $\bar{g}_-|g_+$ assignment tends to change to one of the adjoining conformational domains. It may be noted that the simple "selection rules" established previously[10] for the interdiads of polyisobutylene (PIB) hold for PMMA as well.

The most conspicuous result of the analysis of model I is the suppression of the intrinsically threefold character of the torsional rotation χ_2 in compounds of the kind $X_3CCOOCH_3$. Figure 4 shows plots of the minimum energy obtained within the assigned domain vs. χ_2 for 3 of the 21 independent backbone conformations. The calculated curves for most of the eligible conformations are characterized by two well-defined minima in the vicinity of 0° and 180° and separated by barriers of 4–5 kcal/mol or more. The only exceptions are the $t_-|g_+$ (shown in Figure 4) and the $g_-|\bar{g}_-$ conformations (not shown), for which three minima were found, the minimum near χ = 180° being replaced by two minima on either side of 180°. The energies and approximate values of χ_2 at the minima

Table II
Energies E_{min} and Ester Group Rotations (χ_{min}) at the Minima for Eligible Conformations of Model I

conformation	E_{min} (χ_{min}), kcal mol^{-1} (deg)	
$t_+\|t_+$	0 (0)	1.43 (180)
$t_+\|t_-$	0.11 (0)	1.63 (180)
$t_-\|t_-$	0.26 (0)	1.89 (180)
$t_+\|g_-$	1.98 (0)	3.36 (−150)
$t_+\|g_+$	1.78 (0)	2.98 (−160)
$t_-\|g_-$	1.51 (0)	2.94 (160)
$t_-\|g_+$	1.44 (0)	3.02 (−160)
		3.02 (140)
$t_-\|\bar{g}_-$	4.19 (20)	3.08 (−160)
$t_+\|\bar{g}_-$	3.15 (30)	0.49 (−130)
$t_+\|\bar{g}_+$	2.63 (30)	0.57 (−140)
$t_-\|\bar{g}_+$	3.35 (20)	3.45 (−160)
$g_-\|\bar{g}_-$	5.32 (40)	3.56 (−120)
		5.46 (120)
$g_-\|\bar{g}_+$	5.30 (20)	4.10 (−120)
$g_+\|\bar{g}_+$	6.98 (20)	5.39 (−130)

are summarized in Table II, with the energies referred to the $t_+|t_+$ conformation as the state of reference.

Inasmuch as the energy $E(\chi)$ generally exhibits minima near $\chi = 0$ and π, it is expedient to distinguish these two states by a subscript, 0 or π, appended to the vertical bar denoting the interdiad junction, e.g., as in $t|_\pi g$. It is to be understood that χ may depart appreciably from the indicated values, 0 or π. Such departures are substantial when the state for one of the adjoining bonds is g, and especially when it is $\bar{g}$; see Table II. In the latter case, the value of χ_2 that minimizes the energy is displaced in the direction such that the plane of the ester group is nearly perpendicular to the plane defined by the C–C* bond and the $\bar{g}$ bond. The displacement is substantially higher in the $g|_\pi\bar{g}$ and $\bar{g}|_\pi g$ conformations, in which the carbonyl oxygen eclipses the g bond.

Models IIa and IIb. The same bond geometry was employed in calculations on the trimers IIa and IIb shown in Figure 3. Coulombic interactions, operative in these models, were included. The backbone torsion angles ϕ_2 and ϕ_2' were assigned starting values corresponding to conformations permitted by the rules established above, and ϕ_1 and ϕ_3 were placed in staggered states chosen from t, g, and $\bar{g}$. In some cases the opposite procedure was adopted; that is, ϕ_1' and ϕ_3 were assigned while ϕ_2 and ϕ_2' were placed in permissible staggered states. For each conformation of the backbone, the torsion angle χ_2 was set at an appropriate initial value according to Table II. The external ester groups were given initial orientations χ of 0° or 180°, unless otherwise dictated by the backbone torsion angles. The intramolecular energy was then minimized with respect to all of the torsion angles specified above and to rotations of the methyl groups. In order to reduce end effects, the external ester groups were allowed to shift no more than 30° in either direction with respect to their initial placements. As before, the backbone torsion angles initially assigned to a given conformation (ϕ_2 and ϕ_2' in some case, ϕ_1' and ϕ_3 in others) were confined to their respective domains.

Table III records values of the minimum energy and of relevant torsion angles at these minima for representative conformations selected from those of lower energy for both isotactic and syndiotactic trimers, with the external ester groups in the $\chi \approx 0$ orientation in each instance. The isotactic $t_+t_-|_\pi t_+t_-$ state is taken as reference. Given the preliminary character of these calculations and the large number of conformations examined, the accuracy of the minimizing routine was deliberately kept low. Roughly estimated uncertainties for the data in Table III are ±3°

Table III
Energies (kcal mol^{-1}) and Torsional Angles (deg) at the Minima for Representative Conformations for Isotactic and Syndiotactic Trimers, IIa and IIb

designation $\phi_1\phi_2\|_{\chi_2}\phi_2'\phi_3$	E, kcal mol^{-1}	skeletal conformation, deg ϕ_1	ϕ_2	ϕ_2'	ϕ_3	χ_2, deg
		Isotactic				
$t_+t_-\|_\pi t_+t_-$	0	5	−24	20	−16	167
$t_+t_-\|_\pi t_+g_-$	−0.67	4	−25	8	105	167
$t_-g_+\|_0 t_-g_+$	0.04	−18	128	−15	133	6
$t_+\bar{g}_-\|_\pi t_+t_-$	−3.54	8	−130	12	−15	135
$t_+\bar{g}_-\|_\pi t_+g_-$	−2.20	8	−130	13	108	138
$t_+\bar{g}_-\|_\pi t_+\bar{g}_-$	0.82	7	−132	10	−136	143
$t_-g_+\|_0 t_-\bar{g}_+$	1.42	−20	130	−12	−106	−8
$t_+g_-\|_\pi t_+g_-$	2.29	2	97	7	105	164
$g_-g_+\|_\pi t_-t_+$	3.54	108	132	−18	12	178
$t_-g_+\|_\pi t_-\bar{g}_+$	3.25	−15	131	−16	135	−176
$t_+\bar{g}_-\|_\pi t_-t_+$	3.53	12	−131	−8	30	138
$t_-t_+\|_\pi t_+t_-$	7.30	−18	19	19	−18	179
		Syndiotactic				
$t_+t_+\|_0 t_+t_+$	−7.48	10	8	8	10	0
$g_+t_+\|_0 t_+t_+$	−2.22	138	6	8	14	0
$t_+t_+\|_0 t_-g_-$	−2.20	10	8	−19	111	10
$t_+t_+\|_0 t_-\bar{g}_-$	5.54	22	6	−8	−150	4
$t_+g_+\|_\pi t_-\bar{g}_-$	4.55	6	133	−11	−143	174
$\bar{g}_+t_+\|_0 t_-g_-$	3.79	−102	4	−19	112	12
$t_-\bar{g}_-\|_0 t_+t_+$	4.40	−10	−140	14	6	−40
$g_+g_+\|_\pi t_-t_-$	4.95	132	133	−13	−9	178
$g_-\bar{g}_-\|_0 t_+t_+$	3.14	107	−130	17	5	−45

for the torsion angles and ±0.2 kcal/mol for the energies.

Whatever the starting orientations of the ester groups, the backbone torsion angles were always found to conform to the rule that rotations about successive bonds of a diad sustain displacements from staggered states of the same absolute sense. Exceptions were found only for conformations with energies greater than 15 kcal/mol and for which at least one of the backbone torsion angles reached the limit of its assigned domain. Inasmuch as the skeletal bonds of an isotactic diad are of opposite chirality, departures of the same absolute sense from perfect staggering of bonds is expressed by different subscripts + and −, e.g., by $|t_-t_+|$, $|g_+\bar{g}_-|$, etc.; see Figure 2. In syndiotactic diads the same subscript, + or −, applies to both bonds of the diad according to the rule enunciated above, inasmuch as both bonds are of the same chirality, *d* or *l*.

The two separate minima of the energy found for $t_-|g_+$ in model I with $\chi = 140°$ and $\chi = -160°$ respectively turn out be a single minimum in models IIa and IIb; the same conformation with χ close to 180° is obtained with the two different starting points. The case $g_-|\bar{g}_-$ is more complicated since the orientation of the central ester group in the conformations with minimum energy is markedly dependent on ϕ_1' and ϕ_3. These conformations are, however, always located at the limits of the assigned domain, usually with ϕ_2 at the border separating $\bar{g}_-$ from $\bar{g}_+$. The lowest energy obtained inside the domain is of the order of 10 kcal/mol.

On the basis of the observations cited, we assume below that, for all conformations of the chain backbone, the ester groups may be positioned at $\chi = 0°$ or $\chi = 180°$ as *starting points* for the optimizations.

The results reported in Tables II and III deserve further attention. It will be noticed that some of the conformations containing bonds in a $\bar{g}$ state are quite stable for model I and the most stable for model IIa. These conformations were excluded as too high in energy according to ref 1 where the torsion χ was fixed at either 0° or 180°. The reason for the discrepancy is made clear when the curve for the $t|\bar{g}$ conformation in Figure 4 is considered. Even in the absence of hydrogen atoms on the external

isobutyl groups, the energies of the conformations at χ = 0° or χ = 180° are ca. 4.5 kcal/mol. They decrease rapidly, however, when the constraint on χ is removed, reaching minima for χ = 30° and χ = −140°. Correspondingly, χ at the minimum in the energy for the conformation $t_+\bar{g}_-|_\pi t_+t_-$ of the trimer IIa is 135°. These findings are in qualitative agreement with the work of Sundararajan[2] on helical chains of i-PMMA with a two-bond repeat. Sundararajan found a minimum in the energy in the $\bar{g}|t$ region (−75°|−5°) when χ is fixed at −40°.

Calculations on Long Chains with Regularly Repeating Units

Oligomers of PMMA of short chain length are inadequate models for this disubstituted vinyl polymer inasmuch as the internal stress deriving from the large repulsive interactions can be relieved by adjustments at the ends of the oligomeric chains. This has been fully discussed in ref 10 in the case of PIB in which bond angles and torsion angles have been found to be drastically altered by end effects, even in hexamers.

In order to avoid these end effects, we write the intramolecular energy per segment of a very long chain with a regular succession of conformationally identical segments as

$$E = E_c + \sum_{m=0}^{M} (E_{nb})_m \qquad (2)$$

where E_c is the contribution to the energy of a segment from bond angle distortions and inherent torsional potentials, while $(E_{nb})_m$ is the total nonbonded interaction energy of the atoms in segment i with those in segment $i + m$, or in $i - m$ ($m \geq 0$). A segment is simply defined as the portion of the chain containing one or more monomers as needed to meet the requirement of conformational identity. The upper limit M on the summation is chosen such that $(E_{nb})_m$ for $m \geq M$ approaches the constant value dictated by the energy $E(r^*)$ at truncation of the nonbonded interactions; see above.

The scheme has been applied to regular conformations of PMMA (see IIIa and IIIb in Figure 3) with a four-bond conformational repeat. In each calculation the backbone torsion angles ϕ_1, ϕ_1', ϕ_2 and ϕ_2' were assigned starting values in acceptable domains, while χ_1 and χ_2 were set initially at 0° or 180°. The bond angles τ' were given initial values of 124°. Tetrahedral values were assigned to all other bond angles with the exception of those at the sp^2 carbon of the ester group, for which the geometry specified above was adopted. The intramolecular energy was then optimized with respect to all bond angles and all torsion angles in the conformational repeating segment, each degree of freedom being treated independently. Most of the calculations were performed with M = 1 or with M = 4. Differences between the results thus obtained were usually very small; the energies at the minima differed less than 0.1 kcal/mol. Larger differences found in a few instances are due to long-range interactions caused by fictitious conformational periodicity imposed on the chain.

Tables IV and V report values of the energy per segment (i.e., for two chemical units) and of relevant geometrical parameters obtained with M = 1 for many of the conformations available to isotactic and syndiotactic PMMA subject to restriction to a four-bond repeat segment. The isotactic $t_-|_0t_+t_-|_\pi t_+$ conformation is the state of reference for the energies.

Symmetry dictates that for any value of the torsion angles the following conformations repeated throughout the stereoregular chain must have the same energy, opposite reference frames being affixed to d and l backbone bonds and χ_1 and χ_2 being measured in the reference frame of the second bond at each interdiad:

$$\phi_1|(\chi_1)\phi_1'\phi_2|(\chi_2)\phi_2'$$

$$\phi_1'|(-\chi_1)\phi_1\phi_2'|(-\chi_2)\phi_2$$

$$\phi_2|(\chi_2)\phi_2'\phi_1|(\chi_1)\phi_1'$$

$$\phi_2'|(-\chi_2)\phi_2\phi_1'|(-\chi_1)\phi_1$$

The performance of the minimizing routine was checked repeatedly by optimizing symmetry-related conformations. The geometrical characteristics of the resulting conformations and their energies were always virtually indistinguishable.[22]

Segment partition functions z_0 relative to the reference state for each conformation were estimated in the harmonic approximation from the Hessian matrix of the second derivatives; see ref 10. To reduce the time needed for this computation, bond angles were fixed at their values at the minimum, and the second derivatives were evaluated with respect to torsion angles only. The values of z_0 thus obtained are included in Tables IV and V.

The results of these calculations lead to the following generalizations concerning geometrical features of energetically favored conformations of both isotactic and syndiotactic PMMA:

(i) The intradiad bond angle τ' is nearly always 124 ± 1°; it shows no appreciable dependence on the torsional state of the neighboring skeletal bonds.

(ii) The interdiad bond angles τ assume the value of 106° when both of the adjacent backbone bonds are trans, 111° when one is trans and the other is gauche, and 116° when both are gauche.

(iii) The orientation of the ester groups deviates from χ = 0° or χ = 180° only a few degrees except when a $\bar{g}$ conformation occurs at the interdiad; in such cases, the departure is on the order of 30–40°, with the plane of the ester group approximately perpendicular to the plane defined by the C–C* and the $\bar{g}$ bonds.

(iv) The backbone torsion angles in the principal conformations can be classified according to six states located approximately at ϕ = −20° (t_-), 10° (t_+), 100° (g_-), 125° (g_+), −125° ($\bar{g}_-$), and −100° ($\bar{g}_+$).

It is to be noted further that the minimized energy shows no consistent dependence on the orientation of the ester group (0 or π), according to the results in Table IV and likewise in Table V. Even in the $|t_\pm t_\mp|$ conformations for a diad of the isotactic chain where Coulombic interactions are maximal, discrimination between the states with χ_1 = χ_2 = 0 or π and those with opposite assignments for χ_1 and χ_2 is indecisive.[23]

The data in Tables IV and V indicate that the most stable conformations with a four-bond repeat belong to the all-trans class for both isotactic and syndiotactic PMMA chains; see Figure 5. We have shown previously[24] that the isotactic conformation of lowest energy, $t_-|t_+t_-|t_+$, closely corresponds to the 10/1 helix having a pitch of 21.1 Å and identified in the form of a double helix in crystalline i-PMMA.[25]

Syndiotactic PMMA, on the other hand, has thus far been crystallized only in the presence of a solvent, and attempts to remove the latter have led to loss of the crystallinity. Lovell and Windle[26] have compared the wide-angle X-ray patterns of syndiotactic and atactic PMMA with those calculated from various models with a four-bond repeat. They conclude that the predominant conformation in these polymers is all-trans with torsion angles close to those reported in Table V for the most stable conformations. It should be noted, however, that

Table IV
Characteristics of Regular Conformations of Isotactic PMMA with a Four-Bond Repeating Segment

				torsional angles, deg						bond angles, deg			
no.	$\phi_1\|_{\chi_1}\phi_1'\phi_2\|_{\chi_2}\phi_2'$	E, kcal mol^{-1}	ln z_0	ϕ_1	ϕ_1'	ϕ_2	ϕ_2'	χ_1	χ_2	τ_1	τ_2	τ_1'	τ_2'
1	$t_-\|_0t_+t_-\|_\pi t_+$	0	0	−23	11	−22	12	−8	171	106	106	124	124
2	$g_-\|_0t_+t_-\|_0t_+$	0.08	−0.34	94	8	−19	7	4	−8	110	106	123	124
3	$g_-\|_0t_-t_+\|_0t_+$	0.16	0.21	103	−29	7	6	12	−2	111	106	124	124
4	$t_-\|_0t_+t_-\|_0t_+$	0.23	−1.31	−21	14	−21	14	−7	−7	106	106	124	124
5	$g_-\|_0t_+t_-\|_\pi t_+$	0.41	0.19	95	6	−20	8	3	172	110	106	123	124
6	$t_-\|_\pi t_+t_-\|_\pi t_+$	0.41	0.51	−23	11	−23	11	173	173	106	106	124	124
7	$g_-\|_\pi t_-t_+\|_0t_+$	0.54	0.64	104	−29	6	6	−168	−1	111	106	124	124
8	$g_-\|_0t_-t_+\|_\pi t_+$	0.62	0.17	104	−30	8	6	11	179	111	106	124	124
9	$\bar{g}_-\|_\pi t_+t_-\|_0t_+$	0.69	0.29	−128	14	−17	12	138	−20	111	106	125	124
10	$t_-\|_0t_+t_-\|_0g_+$	0.72	0.34	−12	13	−22	120	−7	−6	105	111	124	125
11	$g_-\|_\pi t_-t_+\|_\pi t_+$	0.73	0.23	104	−30	7	6	−169	177	111	106	124	124
12	$g_-\|_\pi t_+t_-\|_0t_+$	0.84	−0.19	95	9	−21	8	−179	−7	110	106	123	124
13	$g_-\|_\pi t_+t_-\|_\pi t_+$	0.85	−0.20	95	7	−21	8	−176	173	110	106	123	124
14	$t_-\|_0g_-t_+\|_0\bar{g}_+$	0.87	−0.11	−20	105	18	−107	−9	28	111	111	125	125
15	$t_-\|_0t_+t_-\|_\pi g_+$	1.03	0.99	−12	11	−23	120	−7	173	106	111	124	126
16	$t_-\|_0g_+t_-\|_0g_+$	1.08	0.88	−17	127	−17	127	−6	−6	111	111	124	124
17	$t_-\|_0g_-t_+\|_\pi\bar{g}_+$	1.10	0.21	−21	106	19	−108	−10	−144	111	111	125	124
18	$g_-\|_0t_+g_-\|_0t_+$	1.10	0.10	98	3	98	3	−2	−2	111	111	124	124
19	$\bar{g}_-\|_\pi t_+\bar{g}_-\|_\pi t_+$	1.24	1.28	−123	16	−123	16	140	140	111	111	124	124
20	$t_-\|_0g_-t_+\|_0g_+$	1.27	0.45	−26	106	2	128	37	37	112	111	124	124
21	$\bar{g}_-\|_0t_+t_-\|_0t_+$	1.35	−0.03	−130	16	−18	12	−39	−18	111	106	125	124
22	$t_-\|_\pi t_-t_+\|_0t_+$	1.40	1.69	−17	−20	9	11	−179	0	106	107	124	124
23	$t_-\|_\pi t_+t_-\|_0g_+$	1.42	0.60	−14	15	−21	122	170	−4	105	111	125	124
24	$\bar{g}_-\|_\pi t_+t_-\|_\pi t_+$	1.52	0.41	−128	12	−17	13	139	156	111	106	125	124
25	$g_-\|_0t_+g_-\|_\pi t_+$	1.60	0.10	97	3	97	3	−2	178	110	110	124	124
26	$\bar{g}_-\|_0t_+t_-\|_\pi t_+$	1.67	0.22	−130	13	−19	12	−35	159	111	106	124	124
27	$t_-\|_\pi g_-t_+\|_0g_+$	1.70	0.26	−28	106	3	126	165	11	111	112	124	124
28	$t_-\|_0g_+t_-\|_\pi g_+$	1.71	1.10	−17	127	−17	127	−5	171	111	110	124	124
29	$\bar{g}_-\|_\pi t_+t_-\|_0g_+$	1.75	0.63	−129	18	−16	129	144	−16	112	111	123	125
30	$t_-\|_0g_-t_+\|_\pi g_+$	1.76	0.62	−26	106	2	128	−13	−169	111	112	124	124
31	$g_-\|_0t_-t_+\|_\pi\bar{g}_+$	1.80	0.45	106	−19	17	−99	21	−146	110	111	124	125
32	$g_-\|_\pi t_+g_-\|_\pi t_+$	1.82	0.01	97	3	97	3	178	178	110	110	124	124
33	$t_-\|_0t_-t_+\|_0t_+$	1.83	0.82	−16	−19	12	15	1	1	107	107	124	124
34	$t_-\|_\pi t_-t_+\|_\pi t_+$	1.94	0.95	−18	−20	10	11	180	180	108	106	124	124
35	$\bar{g}_-\|_0t_+\bar{g}_-\|_\pi t_+$	1.95	1.26	−124	16	−124	15	−33	139	112	111	124	125
36	$t_-\|_\pi g_-t_+\|_\pi\bar{g}_+$	1.98	0.80	−21	106	19	−108	166	−144	111	111	125	124
37	$g_-\|_0t_-t_+\|_0\bar{g}_+$	1.99	0.11	108	−22	21	−103	12	31	110	111	124	125
38	$t_-\|_\pi g_-t_+\|_\pi g_+$	2.06	0.41	−28	−106	3	126	165	−166	110	112	124	125
39	$t_-\|_\pi g_-t_+\|_0\bar{g}_+$	2.10	0.54	−20	105	18	−108	168	29	111	111	125	125
40	$\bar{g}_-\|_0t_+t_-\|_0g_+$	2.23	0.37	−128	20	−16	129	−34	−13	112	111	124	125
41	$t_-\|_\pi g_+t_-\|_\pi g_+$	2.23	1.44	−17	127	−17	127	172	172	110	110	124	124
42	$g_-\|_\pi t_-t_+\|_0\bar{g}_+$	2.39	0.85	109	−22	19	−103	−168	29	110	111	123	125
43	$t_-\|_0t_-t_+\|_0\bar{g}_+$	2.50	1.17	−11	−19	22	−106	2	24	107	111	124	125
44	$\bar{g}_-\|_\pi t_+t_-\|_\pi g_+$	2.55	0.73	−129	14	−14	130	140	143	112	109	124	125
45	$\bar{g}_-\|_0t_+\bar{g}_-\|_0t_+$	2.64	0.59	−128	16	−128	16	−31	−31	112	112	125	125
46	$t_-\|_\pi t_-t_+\|_0\bar{g}_+$	2.66	0.90	−12	−20	21	−104	179	22	107	111	124	125
47	$g_-\|_0t_-t_+\|_0g_+$	2.72	0.10	103	−26	3	129	14	7	111	113	123	126
48	$\bar{g}_-\|_0t_+t_-\|_\pi g_+$	2.72	0.10	−129	16	−129	16	−32	159	112	110	124	125
49	$t_-\|_0t_+g_-\|_0\bar{g}_+$	2.79	−0.11	−16	8	102	−106	−11	34	105	116	125	125
50	$g_-\|_\pi t_+t_-\|_\pi g_+$	2.86	0.17	94	9	−15	125	−173	180	111	112	123	126
51	$g_-\|_\pi t_-t_+\|_\pi\bar{g}_+$	2.89	0.92	106	−20	17	−99	−161	−147	110	111	124	125
52	$g_-\|_0t_-t_+\|_0g_+$	2.89	−0.29	91	−11	13	125	10	0	110	112	123	125
53	$t_-\|_0t_+g_-\|_\pi\bar{g}_+$	3.02	0.17	−15	9	102	−107	−12	−136	105	116	125	125
54	$t_-\|_\pi t_+g_-\|_\pi\bar{g}_+$	3.07	0.64	−16	10	104	−109	163	−137	105	116	125	125
55	$t_-\|_\pi t_+g_-\|_0\bar{g}_+$	3.11	0.14	−16	9	103	−108	166	34	106	116	125	125
56	$t_-\|_\pi t_-t_+\|_\pi\bar{g}_+$	3.43	1.38	−12	−21	22	−106	178	−155	107	111	124	125
57	$\bar{g}_-\|_\pi t_-t_+\|_0t_+$	3.56	1.05	−148	−15	6	2	−165	−6	113	106	124	125
58	$\bar{g}_-\|_\pi t_-t_+\|_\pi t_+$	3.69	0.35	−147	−16	7	2	170	173	114	106	124	125
59	$g_-\|_\pi t_-t_+\|_\pi g_+$	3.83	0.25	104	−26	2	129	−166	−172	111	113	123	126
60	$\bar{g}_-\|_0t_-t_+\|_0t_+$	4.06	0.48	−150	−17	6	1	12	−7	114	106	124	126
61	$t_-\|_0t_-t_+\|_\pi t_+$	4.48	0.34	−14	−18	13	19	2	−178	106	106	125	125
62	$\bar{g}_-\|_0t_-t_+\|_\pi t_+$	4.60	0.43	−150	−17	7	1	10	174	114	105	124	126
63	$t_-\|_0t_+t_-\|_0\bar{g}_+$	4.62	−0.45	−11	21	−12	−98	−13	18	106	110	125	126
64	$g_-\|_0t_-g_+\|_0\bar{g}_+$	5.13	−0.33	106	−29	123	−97	17	48	111	115	126	124
65	$\bar{g}_-\|_0g_-t_+\|_0\bar{g}_+$	5.40	−1.05	−120	100	13	−89	−54	26	117	110	125	125
66	$g_-\|_0\bar{g}_-t_+\|_0g_+$	5.69	−1.20	90	−126	17	121	45	0	116	113	123	127
67	$g_-\|_\pi\bar{g}_+g_-\|_\pi\bar{g}_+$	5.70	−0.56	107	−103	107	−103	−138	−138	116	116	126	126
68	$g_-\|_0\bar{g}_+g_-\|_\pi\bar{g}_+$	6.18	−0.40	106	−102	109	−104	37	−136	117	116	126	126
69	$g_-\|_0\bar{g}_+g_-\|_0\bar{g}_+$	6.49	−0.22	108	−103	108	−103	37	37	117	117	126	126
70	$\bar{g}_-\|_0t_-t_+\|_0g_+$	6.62	0.10	−144	−13	5	130	12	4	113	114	123	127
71	$\bar{g}_-\|_0t_-t_+\|_0\bar{g}_+$	7.47	0.17	−143	−4	14	−107	36	30	113	111	125	128
72	$\bar{g}_-\|_0t_+t_-\|_0\bar{g}_+$	8.43	0.31	−119	34	−10	−75	−41	28	112	109	125	125
73	$t_-\|_\pi\bar{g}_+t_-\|_\pi\bar{g}_+$	8.47	1.21	−9	−77	−9	−77	−162	−162	109	109	125	125
74	$t_-\|_0\bar{g}_+t_-\|_\pi\bar{g}_+$	8.50	0.99	−6	−78	−6	−70	22	−163	109	108	125	125
75	$t_-\|_0g_-g_+\|_0\bar{g}_+$	8.74	−0.76	−10	97	128	−100	−40	52	110	117	128	125
76	$\bar{g}_-\|_0t_-g_+\|_0\bar{g}_+$	9.61	−0.65	−140	−13	128	−101	2	39	113	117	127	127

Table V
Characteristics of Regular Conformations of Syndiotactic PMMA with a Four-Bond Repeating Segment

				torsional angles, deg						bond angles, deg			
no.	$\phi_1\|_{\chi_1}\phi_1'\phi_2\|_{\chi_2}\phi_2'$	E, kcal mol^{-1}	ln z_0	ϕ_1	ϕ_1'	ϕ_2	ϕ_2'	χ_1	χ_2	τ_1	τ_2	τ_1'	τ_2'
1	$t_+\|_0t_+t_+\|_\pi t_+$	−2.73	1.63	9	9	9	9	3	−177	106	106	124	123
2	$t_+\|_0t_+t_+\|_0t_+$	−2.66	1.68	9	9	9	9	0	0	106	106	124	124
3	$t_+\|_\pi t_+t_+\|_\pi t_+$	−2.58	1.35	9	9	9	9	180	180	106	106	123	123
4	$t_-\|_\pi t_+t_+\|_\pi \bar{g}_-$	−1.90	0.34	−14	8	20	−123	171	−138	106	111	124	123
5	$\bar{g}_+\|_0t_+t_+\|_0t_+$	−1.61	0.71	−101	20	7	4	−40	3	111	106	124	124
6	$\bar{g}_+\|_\pi t_+t_+\|_\pi t_+$	−1.59	0.82	−97	17	8	6	138	−175	112	106	124	124
7	$\bar{g}_-\|_0t_+t_+\|_\pi t_-$	−1.39	−0.05	−127	18	9	−15	−37	−173	112	106	124	123
8	$t_-\|_0t_+t_+\|_0\bar{g}_-$	−1.37	0.05	−14	9	17	−128	−8	35	106	112	124	123
9	$\bar{g}_-\|_0t_+t_+\|_\pi\bar{g}_-$	−0.36	0.77	−128	17	16	−128	−36	−144	111	111	124	124
10	$g_+\|_0t_+\bar{g}_+\|_0t_+$	−0.22	−0.20	128	0	−102	17	−11	−27	111	110	124	123
11	$g_-\|_0t_+tt_+\|_0t_-$	−0.13	0.29	101	6	10	−16	−9	15	112	106	125	123
12	$t_-\|_0t_+t_+\|_\pi g_-$	−0.11	0.56	−14	9	7	100	−14	−170	106	111	125	123
13	$\bar{g}_-\|_0t_+t_+\|_0\bar{g}_-$	0.19	0.63	−129	16	16	−129	−34	34	111	111	123	123
14	$g_-\|_0t_+t_+\|_\pi t_-$	0.22	0.32	104	4	10	−13	−9	−164	112	105	125	123
15	$g_-\|_\pi t_+t_+\|_\pi t_-$	0.62	0.33	103	5	10	−13	169	−164	112	106	125	123
16	$g_-\|_0t_+t_+\|_0\bar{g}_-$	0.78	0.27	98	2	17	−124	−4	40	111	112	125	123
17	$\bar{g}_-\|_0t_+g_+\|_\pi t_-$	1.23	0.19	−125	18	128	−8	−26	171	112	110	125	124
18	$\bar{g}_-\|_0t_+g_+\|_0t_-$	1.37	0.64	−126	17	129	−8	−25	−4	112	111	125	124
19	$t_-\|_0g_+t_+\|_0g_-$	1.41	1.47	−12	129	2	104	−4	2	111	112	125	124
20	$\bar{g}_+\|_0t_+\bar{g}_+\|_0t_+$	1.70	−0.59	−100	12	−100	12	−30	−30	111	111	124	124
21	$g_-\|_0t_-t_-\|_0g_-$	1.76	1.20	105	−11	−11	105	0	0	111	111	125	125
22	$g_-\|_0t_-t_-\|_\pi g_-$	2.18	1.58	105	−11	−12	105	2	178	111	111	123	126
23	$t_-\|_\pi g_-t_-\|_\pi g_-$	2.38	1.35	−18	108	−18	108	168	168	111	111	124	124
24	$t_-\|_0t_-\bar{g}_+\|_0g_-$	2.67	−0.49	−19	8	−102	107	−13	−34	106	116	126	124
25	$\bar{g}_+\|_0g_-t_-\|_0g_+$	4.03	−0.62	−105	104	−18	125	−40	−8	116	112	125	125
26	$g_-\|_0\bar{g}_+t_+\|_0g_-$	4.38	−0.08	106	−105	2	101	35	4	116	112	126	124
27	$g_-\|_0\bar{g}_+\bar{g}_+\|_0g_-$	6.31	−0.53	106	−108	−107	104	35	−35	117	116	126	126
28	$t_-\|_0g_-\bar{g}_-\|_0g_-$	8.08	−0.77	−10	97	−125	104	−38	−49	110	117	127	126
29	$g_-\|_0\bar{g}_-t_-\|_0\bar{g}_-$	10.5	−1.18	102	−126	−9	−133	41	11	114	117	127	125
30	$t_-\|_0\bar{g}_-t_-\|_0\bar{g}_-$	11.7	−0.08	−1	−148	−1	−148	6	6	113	113	127	127

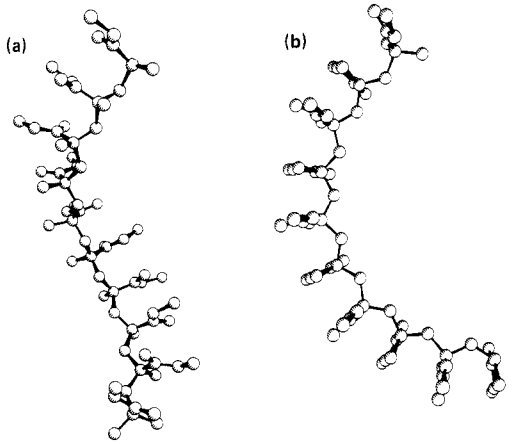

Figure 5. Projections of the conformations of lowest energy for a four-bond segment in (a) isotactic PMMA and (b) syndiotactic PMMA.

the values of the bond angles used in their model (128° and 110° for τ and τ', respectively) differ substantially from the angles indicated by our calculations. The curvature of a syndiotactic sequence in the $t_+|t_+t_+|t_+$ conformation, evident in the projection shown in Figure 5b, has been suggested as a possible cause for the reluctance of s-PMMA to crystallize in the absence of a solvent.[26]

Rotational Isomeric State Analysis

Formulation of a rotational isomeric state scheme that comprehends all aspects of the conformational analysis of PMMA would be a formidable undertaking. Rigorous treatment of the chain in this manner is complicated by the overall lack of symmetry and by the variability of the ester group orientation with respect to surrounding groups.[23] In order to render the task manageable we adopt approximations as follows: (i) interactions of the ester groups are taken to be independent of their torsional states denoted by χ (see above), (ii) interactions within a given diad are considered to be independent of the torsions about bonds beyond those that are first neighbors of the diad considered, and (iii) interactions of CH_2 groups are assumed to be identical with those of CH_3 groups. The first approximation allows specification of the conformation of each skeletal bond in terms of the six states defined in Figure 2. Approximation ii validates use of statistical weight matrices of order 6 × 6, and (iii) reduces the number of statistical weights required. The error due to (iii) is insignificant. Even with these simplifications, the number of statistical weights is fairly large.

Statistical weights for the various interactions of second order (i.e., dependent on torsion angles ϕ for two consecutive skeletal bonds) are denoted by ω for Me···Me, by ν for Me···ester and by ρ for ester···ester interactions. Both CH_2 and CH_3 are included in Me in these designations. Interactions involving an ester group in the orientation dictated by a $\bar{g}$ conformation of one of the adjoining bonds are distinguished by the statistical weights ν' and ρ', respectively. The ester···ester interaction in a meso $|\bar{g}_-\bar{g}_+|$ or $|\bar{g}_+\bar{g}_-|$ diad is denoted by ρ''.

When only second-order interactions are considered, the intradiad matrices for meso and racemic diads are expressed by

$$\mathbf{U}''_m = \begin{vmatrix} 0 & \omega\rho & 0 & \omega\nu & 0 & \nu\nu' \\ & 0 & \omega\nu & 0 & \nu\nu' & 0 \\ & & 0 & \omega^2 & 0 & \omega\nu' \\ & & & 0 & \omega\nu' & 0 \\ & & & & 0 & \omega\rho'' \\ & & & & & 0 \end{vmatrix} \quad (3)$$

and

$$\mathbf{U}''_r = \begin{vmatrix} \nu^2 & 0 & \omega\nu & 0 & \omega\rho' & 0 \\ & \nu^2 & 0 & \omega\nu & 0 & \omega\rho' \\ & & \omega^2 & 0 & \omega\nu' & 0 \\ & & & \omega^2 & 0 & \omega\nu' \\ & & & & \nu'^2 & 0 \\ & & & & & \nu'^2 \end{vmatrix} \quad (4)$$

Table VI
Parameters for the Six-State Scheme

A. Intradiad Parameters (See Eq 5 and 6)

parameter	energy, kcal mol^{-1} (ln z_0)
α	−0.46 (0.09)
$\bar{\alpha}$	−0.77 (−0.04)
β	−3.42 (0.15)
ρ^*	−0.06 (−0.64)
$\bar{\rho}$	−2.14 (−0.44)

B. Interdiad Parameters Arranged in Matrix Form (See Eq 7)

1.80 (1.00)	0. (0.)	4.61 (−0.51)	4.54 (0.32)	5.42 (0.38)	4.67 (0.39)
	−0.47 (0.64)	4.14 (−0.29)	4.49 (0.51)	1.85 (0.58)	1.51 (0.39)
		0	0	9.91 (−1.22)	7.94 (−0.06)
			0	0	8.24 (−0.36)
				0	0
					0

respectively, with omission of redundant elements in these symmetric matrices. All first-order interactions are relegated to U′; see below. Rotational isomeric states are indexed in the order t_-, t_+, g_-, g_+, $\bar{g}_-$, $\bar{g}_+$.

The statistical weights may be normalized to unity for the meso t_-t_+ diad. Then, with the substitutions $\alpha = \nu/(\rho\omega)^{1/2}$, $\bar{\alpha} = \nu'/(\rho\omega)^{1/2}$, $\beta = (\omega/\rho)^{1/2}$, $\bar{\rho} = \rho'/\rho$, and $\rho^* = \rho''/\rho$, the number of independent parameters is reduced and the statistical weight matrices are simplified to

$$\mathbf{U'}_m = \begin{vmatrix} 0 & 1 & 0 & \alpha\beta & 0 & \alpha\bar{\alpha} \\ & 0 & \alpha\beta & 0 & \alpha\bar{\alpha} & 0 \\ & & 0 & \beta^2 & 0 & \bar{\alpha}\beta \\ & & & 0 & \bar{\alpha}\beta & 0 \\ & & & & 0 & \rho^* \\ & & & & & 0 \end{vmatrix} \quad (5)$$

and

$$\mathbf{U'}_r = \begin{vmatrix} \alpha^2 & 0 & \alpha\beta & 0 & \bar{\rho} & 0 \\ & \alpha^2 & 0 & \alpha\beta & 0 & \bar{\rho} \\ & & \beta^2 & 0 & \bar{\alpha}\beta & 0 \\ & & & \beta^2 & 0 & \bar{\alpha}\beta \\ & & & & \bar{\alpha}^2 & 0 \\ & & & & & \bar{\alpha}^2 \end{vmatrix} \quad (6)$$

It will be noted that the parameters α and β comprise second-order statistical weights exclusively. They are unrelated to the quantities α and β defined in ref 1.

The symmetry of these expressions for the intradiad matrices contrasts with the asymmetry inherent in the PMMA chain. This is a consequence of the substantial approximations adopted. For example, the same statistical weight α^2 is attributed to second-order interactions in t_-t_- and in t_+t_+ racemic diads, whereas the t_- and t_+ states are located at −20° and 10°, respectively. Similar incongruities occur for some of the two-bond conformations not mutually related by symmetry. Thus, the various parameters appearing in the intradiad matrices must be considered to represent "average" interactions of second order. A better description is conceivably attainable through the use of additional statistical weights with which to distinguish different conformations. Corresponding elaboration of the interdiad matrix U′ would be required, however. This would lead to an excessive proliferation of parameters.

The interdiad statistical weight matrix, in which we include all first-order interactions, may be written

$$\mathbf{U'} = \begin{vmatrix} u_{t_-t_-} & 1 & u_{t_-g_-} & u_{t_-g_+} & u_{t_-\bar{g}_-} & u_{t_-\bar{g}_+} \\ & u_{t_+t_+} & u_{t_+g_-} & u_{t_+g_+} & u_{t_+\bar{g}_-} & u_{t_+\bar{g}_+} \\ & & 0 & 0 & u_{g_-\bar{g}_-} & u_{g_-\bar{g}_+} \\ & & & 0 & 0 & u_{g_+\bar{g}_+} \\ & & & & 0 & 0 \\ & & & & & 0 \end{vmatrix} \quad (7)$$

with elements normalized to $u_{t_-t_+} = u_{t_+t_-} = 1$. The null elements reflect the rules adduced from the analysis of model I. There are 13 independent, nonzero elements in eq 7.

Following the procedure of ref 10, we have solved (in the least-squares sense) the two overdetermined systems of 106 equations and 19 unknowns (18 independent statistical weights plus the reference state) that are obtained when E and ln z_0 for each of the conformations in Tables IV and V are written in terms of additive contributions from the appropriate E_η and η_0 in the general equation

$$\eta = \eta_0 \exp(-E_\eta/RT), \qquad \eta = \alpha, \beta \ldots u_{t_-t_-} \ldots \quad (8)$$

Each equation in the two systems of equations was weighted by $w = z_0 \exp(-E/RT)$ with $T = 300$ K. Separate sets of weights were used for isotactic and for syndiotactic chains, both being normalized to unity for the two respective conformations with lowest energy. Values of E_η and ln η_0 for the various statistical weights are reported in Table VI.

The agreement between E_a and ln z_a determined on the hypothesis of additivity according to the results in Table VI on the one hand and, on the other, according to the values of these quantities calculated directly from the computed conformational energies given in Tables IV and V is generally satisfactory. Values of $\langle w^2(E - E_a)^2\rangle^{1/2}$ are ca. 0.05 kcal/mol and those of $\langle w^2(\ln z_0 - \ln z_a)^2\rangle^{1/2}$ coincidentally approximate 0.05 also. The good agreement suggests that interactions of order higher than the second and long-range correlations either are of low incidence in the most stable conformations of PMMA or tend to compensate one another. We have found that the inclusion of three more parameters in order to distinguish between the 0 and π orientations of the ester groups (which leads to a less tractable 12-state model) reduces the weighted root-mean-square deviations only from 0.05 to 0.04.

The a priori probabilities for the six-bond conformations at 300 K, with states indexed in the order above, are

$$P_i = |0.298\ 0.420\ 0.138\ 0.059\ 0.063\ 0.021|$$

for the isotactic polymer and

$$P_s = |0.052\ 0.834\ 0.005\ 0.025\ 0.012\ 0.072|$$

for the syndiotactic polymer. In both cases about 8% of the chain bonds are in $\bar{g}$ states and the trans conformation is preferred. The syndiotactic polymer shows a much stronger preference for the t_+ state, however. This preference is even more pronounced when the probability of occurrence of two consecutive bonds in various states is examined. Thus, the fraction of diads occurring in each of the mirror-related conformations $|t_-t_+|$ and $|t_+t_-|$ in the isotactic polymer is 0.228. In the syndiotactic chain, the fraction of the diads occurring in the $|t_+t_+|$ conformation

is 0.739 compared with only 0.037 for $|t_-t_-|$. A similar trend is observed at the interdiads, where the fraction of $t_+|t_+$ conformations is 0.680 in the syndiotactic chain, with all the other t|t interdiads adding up to only 0.092. In contrast, the t|t interdiads occurring in the isotactic PMMA chain are almost evenly distributed among the four possible combinations. The total average length of a trans sequence is about seven units for syndiotactic chains, compared with less than two units in the isotactic chain.

The a priori probability of a trans bond, inclusive of both t_- and t_+, is 0.72 for i-PMMA and 0.89 for s-PMMA. In the case of PIB, the probability of a trans bond is only 0.50.[10] Furthermore, the incidence of g_- and $\bar{g}_+$ states is negligible in PIB. For this reason a four-state scheme is applicable to PIB.[10] The analysis of PMMA reveals significant occurrence of these states; hence, a corresponding simplification of the six-state scheme is impracticable.

Configuration-Dependent Properties

Evaluation of experimentally measurable configuration-dependent properties of PMMA (such as the characteristic ratio) according to well-known generator matrix methods[21,27] is complicated by the sensitivity of the calculated values to the skeletal bond angles. Since the interdiad angle τ for PMMA varies with the torsional state of the two adjacent bonds, either an "effective" value must be selected (not necessarily coincident with the average) or, preferably, the generator matrices should be altered to take into account this effect. The fraction of t|t conformations at the interdiad, which determines the average value of τ, is ca. 0.44 for i-PMMA and ca. 0.77 for s-PMMA, both at 300 K. Hence, an "effective" value of τ must be expected to vary both with temperature and with stereochemical structure.

The generator matrix methods are easily adapted to take account of the dependence of τ on conformation.[21,27] For the calculation of the configurational average of a given property f such as the mean-square end-to-end length, the radius of gyration, the dipole moment, etc., it suffices to associate the appropriate generator matrices for the various rotational states of bond $i-1$ with the statistical weight matrix $\mathbf{U}_i$ for bond i instead of with $\mathbf{U}_{i-1}$. With this revision the version of eq 51 of ref 27 that applies to evaluation of the mean-square end-to-end length $\langle r^2 \rangle$ of the chain can be recast as

$$\langle r^2 \rangle = \mathbf{Z}^{-1}\mathbf{C}^*(\mathbf{U}_1 \otimes \mathbf{E}_s)[\prod_{i=2}^{n} \|\mathbf{G}_{i-1}\|(\mathbf{U}_i \otimes \mathbf{E}_s)]\|\mathbf{G}_n\|\mathbf{C} \quad (9)$$

where successive bonds of the chain are serially indexed from 1 to n (i.e., for i even, $i/2$ equals index k used above), $\mathbf{U}_1$ and $\mathbf{U}_n$ for the terminal bonds of the chain are identities of the order equal to the number ν of rotational states, the $\mathbf{G}_i$ are generator matrices,[21,27] serial multiplication of which leads to r^2 for a specified conformation, $\mathbf{E}_s$ is the identity of the same order s as the $\mathbf{G}_i$, $\mathbf{C}^*$ is the row [1, 0, 0 ... 0] of order νs, where ν is the number of rotational states, and $\mathbf{C}$ is the column $\mathbf{C}$ = col [$\mathbf{C}'$, $\mathbf{C}'$, ...] of the same order, with $\mathbf{C}'$ = col [0, 0, ... 1] of order s. The generator matrices $\mathbf{G}_i$ are defined in ref 21 and 27. They depend on the transformation $\mathbf{T}_i$ from the reference frame for bond $i+1$ to that for bond i. The $\mathbf{T}_{i-1}$ in the $\mathbf{G}_{i-1}$ of the array $\|\mathbf{G}_{i-1}\|$ for even values of i depend not only on ϕ_{i-1} but also on the bond angle τ_i at C_k^α, where $k = i/2$. Through association on the $\mathbf{G}_{i-1}$ for various rotational states of bond $i-1$ with $\mathbf{U}_i$ as in eq 9, allowance for the dependence of τ_k on the rotational states of the two successive interdiad skeletal bonds is straightforward.

The value $\tau = 106°$ was used for the interdiad bond angle when both adjacent backbone bonds are in a trans state; 111° was employed for all other conformations. The intradiad angle τ' was fixed at 124° throughout. Characteristic ratios thus calculated for the isotactic and syndiotactic polymers at 300 K are 10.3 and 7.3, respectively. Calculations in which the interdiad angle was taken to be tetrahedral also yielded 10.3 for the isotactic polymer but the much larger value 9.3 for the syndiotactic polymer at 300 K. The drastic effect of the interdiad bond angle τ in the latter case is apparent.

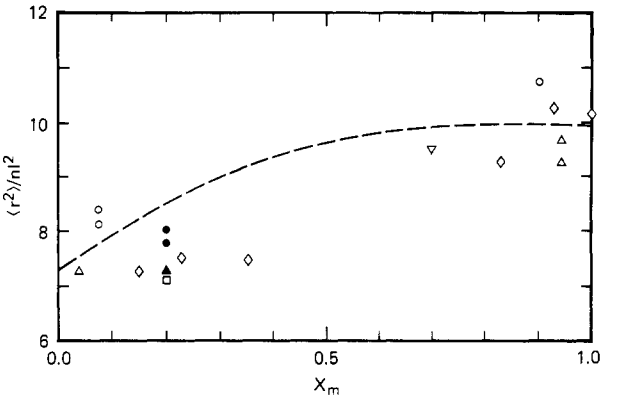

Figure 6. Comparison of the curve representing characteristic ratios calculated as a function of stereochemical constitution, expressed by the fraction X_m of meso diads, with experimental results shown by points from sources as follows: (○) ref 28; (△) ref 29; (◇) ref 31; (▽) ref 32; (□) ref 33; (●) ref 34; (▲) ref 35.

Temperature coefficients calculated from the parameters in Table VI at 300 K are -2×10^{-4} K^{-1} and 2×10^{-3} K^{-1} for i-PMMA and s-PMMA, respectively, in qualitative agreement with experimental evidence from various sources, suggesting a negative value for i-PMMA[28] and a large, positive value, on the order of 1×10^{-3}–4×10^{-3} K^{-1}, for s-PMMA.[28-30]

Characteristic ratios $\langle r^2 \rangle / nl^2$ evaluated according to the six-state scheme are shown by the curves in Figure 6 as a function of stereochemical composition; experimental data from various sources,[28,29,31-35] are indicated by the points. Calculations were performed for chains consisting of 200 units generated by Monte Carlo methods, the distribution of meso and racemic diads being Bernoullian. The calculated curve is seen to fall in the experimental range when the statistical weights are evaluated from the parameters in Table VI. However, it is convex with stereochemical composition rather than concave, as the experimental points suggest. The curvature conforms to previous calculations.[1] The curve cannot be rendered concave by any reasonable adjustment of the parameters that preserves the approximate agreement with the magnitude of the characteristic ratios observed. The scatter of the experimental points obtained by various methods and the lack of precise information on the stereochemical composition of the polymers in some cases preclude definitive conclusions on the reality of this indicated minor disparity between calculations and experiments. It may be significant that the recent work of Jenkins and Porter,[31] in which the unperturbed dimensions have been determined for polymers with well-characterized stereochemical composition, seems to suggest a linear or only slightly concave relationship.

Figure 7 shows plots of $\langle r^2 \rangle / nl^2$ for i-PMMA and s-PMMA against $2/n$, the reciprocal of the number of units in the chain. The appearance of a broad maximum in the curve for s-PMMA located in the range n = 20–24 contrasts with the usual monotonic increase of this ratio toward its asymptote found for other polymers, i-PMMA included. It is related to the tendency of the chain tra-

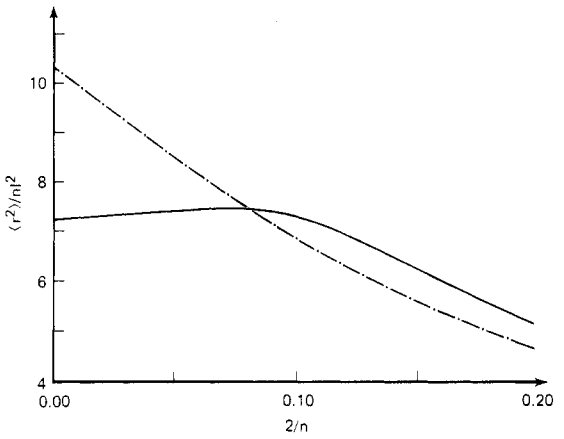

Figure 7. Characteristic ratios $\langle r^2\rangle_0/nl^2$ calculated for finite chains as functions of the reciprocal of the number of units, $2/n$. Isotactic PMMA (-·-); syndiotactic PMMA (—).

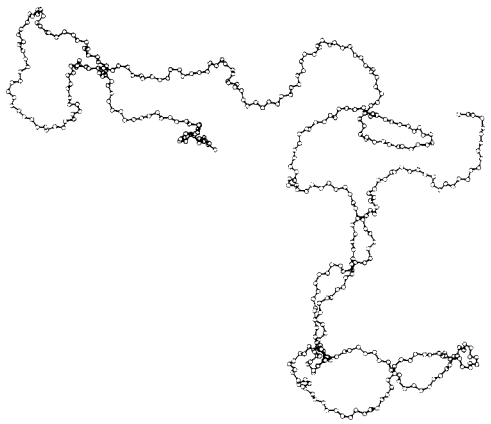

Figure 8. Projection of a Monte Carlo i-PMMA chain consisting of 400 bonds.

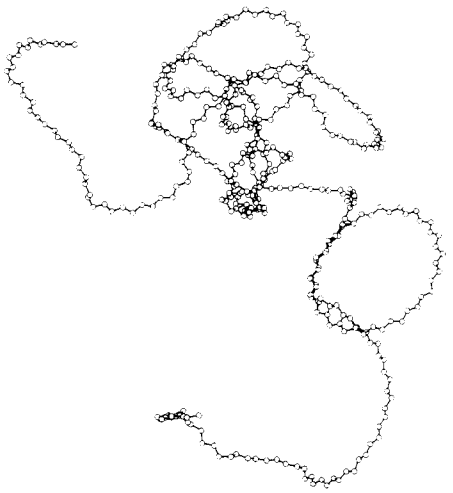

Figure 9. Projection of a Monte Carlo s-PMMA chain consisting of 400 bonds.

jectory to circle back on itself, causing the distances between units separated by m intervening units to decrease with m over the range indicated.[36]

Projections of the trajectories of Monte Carlo chains of i-PMMA and s-PMMA are shown in Figures 8 and 9, respectively. The tendency for the s-PMMA chain to proceed along quasi-cyclic paths is evident in Figure 9. This propensity is a direct consequence of the perpetuation of $t_+|t_+t_+|t_+$ sequences, readily discernible in the figure. The presence of a maximum in the Kratky plot of the X-ray[37] and neutron[38] scattering intensities for s-PMMA in the range 0.05–0.10 Å^{-1} of the scattering vector has been shown[36] to be related to this characteristic of the s-PMMA chain configuration.

Acknowledgment. We acknowledge the advice and suggestions of Dr. Do Y. Yoon throughout the course of this work. We are grateful also to Dr. P. R. Sundararajan for kindly making available to us a copy of his manuscript on "Conformational Analysis of Poly(methyl methacrylate)" submitted concurrently with this paper. It parallels our treatment in a number of respects. It differs, however, in regard to the assignment of bond angle τ and in the use of a three-state scheme. M.V. thanks IBM World Trade of Italy for providing a postdoctoral fellowship.

Registry No. PMMA (homopolymer), 9011-14-7; isotactic-PMMA (homopolymer), 25188-98-1; syndiotactic-PMMA (homopolymer), 25188-97-0.

References and Notes

(1) Sundararajan, P. R.; Flory, P. J. *J. Am. Chem. Soc.* **1974**, *96*, 5025.
(2) Sundararajan, P. R. *Macromolecules* **1979**, *12*, 575.
(3) Havriliak, S.; Roman, N. *Polymer* **1966**, *7*, 387.
(4) Schneider, B.; Stokr, J.; Dirlikov, D.; Mihailov, M. *Macromolecules* **1971**, *4*, 715.
(5) McCrum, N. G.; Read, B. E.; Williams, G. "Anelastic and Dielectric Effects in Polymers"; Wiley: New York, 1967; pp 238–255.
(6) Conventions on signs of torsional angles introduced in ref 7 are followed here. Thus, right- and left-handed reference frames are chosen for skeletal bonds according to their intrinsic chirality. The torsion angle ϕ is measured in the corresponding sense.
(7) Flory, P. J.; Sundararajan, P. R.; DeBolt, L. C. *J. Am. Chem. Soc.* **1974**, *96*, 5015.
(8) O'Reilly, J. M.; Mosher, R. A. *Macromolecules* **1981**, *14*, 602.
(9) O'Reilly, J. M.; Teegarden, D. M.; Mosher, R. A. *Macromolecules* **1981**, *14*, 1693.
(10) Suter, U. W.; Saiz, E.; Flory, P. J. *Macromolecules* **1983**, *16*, 1317.
(11) Yoon, D. Y.; Suter, U. W.; Sundararajan, P. R.; Flory, P. J. *Macromolecules* **1975**, *8*, 784.
(12) Hummel, J. P.; Flory, P. J. *Macromolecules* **1980**, *13*, 479.
(13) Abe, A.; Jernigan, R. L.; Flory, P. J. *J. Am. Chem. Soc.* **1966**, *88*, 631.
(14) Allinger, N. L.; Chang, S. *Tetrahedron* **1977**, *33*, 1561.
(15) Yan, J. F.; Vanderkooi, G.; Scheraga, H. A. *J. Chem. Phys.* **1968**, *49*, 2713.
(16) Williams, G.; Owen, N. L.; Sheridan, J. *Trans. Faraday Soc.* **1971**, *67*, 922.
(17) Lister, D. G.; MacDonald, J. N.; Owen, N. L. "Internal Rotation and Inversion"; Academic Press: New York, 1978.
(18) Ooi, T.; Scott, R. A.; Vanderkooi, G.; Scheraga, H. A. *J. Chem. Phys.* **1967**, *46*, 4410.
(19) Saiz, E.; Hummel, J. P.; Flory, P. J.; Plavsic, M. *J. Phys. Chem.* **1981**, *85*, 3211.
(20) Bond angles τ are used instead of their supplements denoted by θ elsewhere.[21] Thus, $\tau = \pi - \theta'$ and $\tau' = \pi - \theta''$, where θ' and θ'' are the bond angle supplements used previously[1,7,10,21] for the analysis of the configurations of vinyl polymer chains.
(21) Flory, P. J. "Statistical Mechanics of Chain Molecules"; Wiley-Interscience: New York, 1969.
(22) In several instances, especially for the syndiotactic polymer, the conformation initially assigned to the backbone changed to a different domain during the optimization process. These conformations are not reported in the tables and have not been used in the following calculations. Changes from the assigned domains to the new one nearly always were cooperatively correlated so that the resulting conformation obeys the previously established selection rules; for instance, the syndiotactic $t_-|t_-t_-|t_-$ changed to $t_+|t_+t_+|t_+$ and $\bar{g}_-|t_-t_-|\bar{g}_-$ changed to $\bar{g}_-|t_+t_+|\bar{g}_-$. In a few cases, however, the final result was a "forbidden" conformation in contradiction of the intradiad rules, involving, for example, a change of bond torsion from t_- to t_+, or vice versa. The energies in all the cases were greater than 2.5 kcal/mol.
(23) The positioning of an ester group relative to the chain backbone depends on the torsional states of *both* skeletal bonds flanking the C^α at the interdiad. The full array of interactions

involving ester group k depends therefore on the torsional angles of skeletal bonds within both of the adjoining diads and on χ_{k-1} and χ_{k+1} as well as on χ_k. A complete accounting of the influences of these parameters incident to a given ester group would be beyond reach of any manageable treatment.
(24) Vacatello, M.; Flory, P. J. *Polym. Commun.* **1984**, *25*, 258.
(25) Kusanagi, H.; Tadokoro, H.; Chatani, Y. *Macromolecules* **1976**, *2*, 531.
(26) Lovell, R.; Windle, A. H. *Polymer* **1981**, *22*, 175.
(27) Flory, P. J. *Macromolecules* **1974**, *7*, 381.
(28) Sakurada, I.; Nakajima, A.; Yoshizaki, O.; Nakamae, K. *Kolloid Z.* **1962**, *186*, 41.
(29) Shulz, G. V.; Wunderlich, W.; Kirste, R. *Makromol. Chem.* **1964**, *75*, 22.
(30) Moore. W. R.; Fort, R. F. *J. Polym. Sci., Part A* **1963**, *1*, 929.
(31) Jenkins, R.; Porter, R. S. *Polymer* **1982**, *23*, 105.
(32) Krause, S.; Cohn-Ginsberg, E. *J. Phys. Chem.* **1963**, *67*, 1479.
(33) Vadusevan, P.; Santappa, M. *J. Polym. Sci., Part A-2* **1971**, *9*, 483.
(34) Chinai, S. N.; Valles, R. J. *J. Polym. Sci.* **1959**, *39*, 363.
(35) Fox, T. G. *Polymer* **1962**, *3*, 111.
(36) Yoon, D. Y.; Flory, P. J. *Macromolecules* **1976**, *9*, 299.
(37) Kirste, R. G. *Makromol. Chem.* **1967**, *101*, 91.
(38) Kirste, R. G.; Kruse, W. A.; Ibel, K. *Polymer* **1975**, *16*, 120.

Conformational Analysis of Poly(methyl methacrylate)

P. R. Sundararajan

Xerox Research Centre of Canada, 2660 Speakman Drive, Mississauga, Ontario L5K 2L1, Canada. *Received April 2, 1985*

ABSTRACT: Conformational energies associated with the various states of the meso and racemic diads of poly(methyl methacrylate) have been estimated. The skeletal bond angle at the methylene carbon atom and the side-group torsion angles were varied in order to minimize the energy at each of the skeletal conformations defined by φ_i and φ_{i+1}. In contrast to the previous calculations with fixed side-group torsion angles, the present results show that the $\bar{g}$ conformation is accessible to the chain. Agreement between the experimental and theoretical values of the characteristic ratio $\langle r^2\rangle_0/nl^2$, for the isotactic chain, is achieved if the tt state is treated with $(\varphi_i, \varphi_{i+1}) = (10°, -15°)$, leading to helical segments with a large pitch. The energy differences between the various states estimated from the calculations are compared with the values derived from FTIR experiments.

Introduction

Calculations on the conformational energies of the various states accessible to the poly(methyl methacrylate) (PMMA) chain have been reported by Sundararajan and Flory.[1,2] The $\bar{g}$ state was ruled out, leading to a two-state scheme (involving t and g) for the formulation of the statistical weight matrices and the calculation of the characteristic ratio and its temperature coefficient. The energy parameters derived from this work have been used by various authors to calculate properties of the PMMA chain such as the small-angle X-ray and neutron scattering curves,[3] wide-angle X-ray scattering[4] from amorphous PMMA, the average dipole moment,[5] persistance vectors,[6] etc. The characteristic ratios calculated for the stereoirregular chains have been compared with recent experimental results.[7,8]

While calculations such as the characteristic ratios and scattering curves depend on the energy parameters derived from conformational analysis, direct derivation of differences in energies between various states of the chain has been reported by O'Reilly and co-workers,[9,10] using FTIR methods. Measurements were carried out on both hydrogenated and deuterated isotactic, syndiotactic, and atactic PMMA. The energies were assigned on the basis of the two-state (tt and tg/gt) model. It was also possible to separate the energies associated with the backbone and side chains. The agreement with previous calculations was good in the case of syndiotactic PMMA but not for the isotactic case.[9] Further, the experiments on deuterated PMMA prompted the suggestion[10] that additional gauche states might be accessible to PMMA.

Considering the active interest in the estimation of energy differences between various states of PMMA, arising from short-range interactions, the calculations of conformational energies were reexamined. Allowance was made for the variation of the skeletal bond angle $C^\alpha CC^\alpha$ and the side-group torsion angles. The present calculations indicate the accessibility of additional states when variations in such geometrical parameters are taken into account.

Description of Calculations

The various geometrical parameters are defined in the schematic shown in Figure 1. The bond lengths and bond angles were chosen as before[1] except that the angle θ'' was varied from 118 to 126°, in steps of 2°, at each of the $(\varphi_i, \varphi_{i+1})$ conformations. The enlargement of the angle θ'' from tetrahedral value, in order to accommodate the large size of the side groups, has been discussed before.[1] The CH_2 and CH_3 groups were treated as hard spheres except for the methylene group $(CH_2)_i$. As the value of θ'' was varied from 118° to 126°, for each θ'', the two hydrogen atoms of the methylene group were located such that the angles $C^\alpha_{i-1}C_iH_i$, $C^\alpha_{i-1}C_iH_i$*, $C^\alpha_{i+1}C_iH_i$, $C^\alpha_{i+1}C_iH_i$* and $H_iC_iH_i$* are equal and denoted by θ. Modification of eq 2 of Suter and Flory[11] to this end leads to

$$\cos\theta = \frac{1 \pm (1 + 4x)^{1/2}}{2x} \tag{1}$$

where

$$x = 4/(1 + \cos\theta'') \tag{2}$$

The side-group torsion angles χ_{i-1} and χ_{i+1} were taken to be 0° when the carbonyl bond eclipses the C^α–CH_3 bond. The angles χ_{i-1} and χ_{i+1} were varied, in steps of 10^0 in the ranges of −40° to +40° and 140° to 220°, corresponding to the "up" and "down" configurations of the carbonyl bond. Values of χ outside these ranges were considered unlikely. (This restriction gave rise to a problem in certain conformations such as $\bar{g}\bar{g}$. A well-defined minimum for (χ_{i-1}, χ_{i+1}) was not reached within the above range in these cases. Further analysis showed that a minimum is reached about 10° beyond the above range, although the energy decreased by only a few cal mol^{-1}. In such cases, the least energy corresponding to the extremities of the above range

0024-9297/86/2219-0415$01.50/0